BRNO UNIVERSITY OF TECHNOLOGY
VYSOKÉ UČENÍ TECHNICKÉ V BRNĚ

FACULTY OF INFORMATION TECHNOLOGY
FAKULTA INFORMAČNÍCH TECHNOLOGIÍ

DEPARTMENT OF COMPUTER GRAPHICS AND MULTIMEDIA
ÚSTAV POČÍTAČOVÉ GRAFIKY A MULTIMÉDIÍ

ANALYSIS OF LANDSCAPE DEFORESTATION USING SATELLITE IMAGERY

ANALÝZA DEFORESTACE KRAJINY S VYUŽITÍM SATELITNÍCH SNÍMKŮ

BACHELOR'S THESIS
BAKALÁŘSKÁ PRÁCE

AUTHOR **MARTIN JAVORKA**
AUTOR PRÁCE

SUPERVISOR **Ing. VÍTĚZSLAV BERAN, Ph.D.**
VEDOUCÍ PRÁCE

BRNO 2020

Vysoké učení technické v Brně
Fakulta informačních technologií

Ústav počítačové grafiky a multimédií (UPGM) Akademický rok 2019/2020

Zadání bakalářské práce

23137

Student: **Javorka Martin**
Program: Informační technologie
Název: **Analýza deforestace krajiny s využitím satelitních snímků**
Analysis of Landscape Deforestation Using Satellite Imagery
Kategorie: Zpracování obrazu

Zadání:

1. Seznamte se s problematikou detekce deforestace krajiny analýzou satelitních snímků. Zaměřte se na metody zpracování obrazu a fúze dat.
2. Navrhněte celkový postup, dílčí metody a aplikaci, která bude detekovat a kvantifikovat úbytek lesního porostu. Zaměřte se na řešení vybraných problematických částí existujících řešení.
3. Připravte vhodnou datovou sadu a její anotaci.
4. Implementujte navržené řešení s využitím vhodných knihoven.
5. Vyhodnoťte vlastnosti výsledného systému na základě experimentů s reálnými daty.
6. Prezentujte klíčové vlastnosti řešení formou plakátu a krátkého videa.

Literatura:

- M. Sonka, V. Hlaváč, R. Boyle. *Image Processing, Analysis, and Machine Vision*, CL-Engineering, ISBN-13: 978-0495082521, 2007.
- Gary R. Bradski, Adrian Kaehler. *Learning OpenCV: Computer Vision with the OpenCV Library*, ISBN 10: 0-596-51613-4, September 2008.

Podrobné závazné pokyny pro vypracování práce viz https://www.fit.vut.cz/study/theses/

Vedoucí práce:	**Beran Vítězslav, Ing., Ph.D.**
Vedoucí ústavu:	Černocký Jan, doc. Dr. Ing.
Datum zadání:	1. listopadu 2019
Datum odevzdání:	31. července 2020
Datum schválení:	1. listopadu 2019

Abstract

Today is important to protect forest resources and tracking deforestation is essential. Remote sensing has an important role in this monitoring effort. This thesis studies four different techniques for detecting deforestation from satellite imagery - using both optical and radar data. The specifics of Earth observation data and geospatial analyses are described. The analytical techniques are used for detecting deforestation in the study area of Chočské vrchy. Image segmentation with Unet neural network model is used to classify there all deforested patches.

Abstrakt

Dnes je dôležité chrániť lesné zdroje a sledovať odlesňovanie je nevyhnutné. Diaľkové snímanie Zeme má v tomto monitorovacom úsilí dôležitú úlohu. Táto práca sa zaoberá štyrmi rôznymi technikami zisťovania odlesňovania zo satelitných snímok - pomocou optických aj radarových dát. Sú opísané špecifiká dát pri diaľkovom snímaní Zeme a geopriestorové analýzy. Analytické techniky sa používajú na zisťovanie odlesňovania v študijnej oblasti Chočské vrchy. Segmentácia obrazu pomocou modelu neurónovej siete Unet sa používa na klasifikáciu všetkých odlesnených území.

Keywords

deforestation, satellite imagery, analysis, transfer learning, unet, ndvi, radar

Kľúčové slová

odlesňovanie, satelitné snímky, analýza, transfer learning, unet, ndvi, radar

Reference

JAVORKA, Martin. *Analysis of Landscape Deforestation Using Satellite Imagery.* Brno, 2020. Bachelor's thesis. Brno University of Technology, Faculty of Information Technology. Supervisor Ing. Vítězslav Beran, Ph.D.

Rozšírený abstrakt

Diaľkové snímanie Zeme je zhromažďovanie informácií o povrchu pomocou satelitov. Satelity na pozorovanie Zeme zhromažďujú aj informácie, ktoré nie sú voľným okom viditeľné. S údajmi na diaľkové snímanie môžeme vykonávať merania zemského povrchu v globálnom meradle a tiež na akomkoľvek konkrétnom mieste vo veľmi vysokom rozlíšení.

V prvej časti práce sme sa pozreli na vlastnosti satelitných dát. Popísané sú špecifiká multi-spektrálnych dát; ukážku vegetačného indexu NDVI; parametre radarových dát; súradnicový referenčný systém a projekcie; a neurónové siete.

Na detekovenie odlesnovania boli použité 4 metódy. Všetky porovnávajú zisten výsledky s údajmi s datasetu Global Forest Change.

Prvá metóda porovnáva hodnoty z vegetačného indexu NDVI medzi rôznymi obdobiami. Ďalšie dve sledujú zmeny v časovej sérii radarových snímok. Odlesné územia boli detekované aj pomocou neurónovej siete s architektúrou UNet.

Analysis of Landscape Deforestation Using Satellite Imagery

Declaration

I hereby declare that this Bachelor's thesis was prepared as an original work by the author under the supervision of Ing. Vítězslav Beran Ph.D. I have listed all the literary sources, publications and other sources, which were used during the preparation of this thesis.

. . . .
Martin Javorka
July 31, 2020

Acknowledgements

I would like to thank my supervisor Ing. Vítězslav Beran Ph.D. for his willingness during the consultations, guidance, and mainly for his patience throughout the course of the work on this thesis.

Contents

Chapter 1

Introduction

In the European Union (EU), forests account for approximately 38% of the total land surface and are supporting life on Earth[8]. Forests support biodiversity, play an important role in the global carbon cycle, and are important in a wide range of economic activities.

Deforestation comes at an enormous cost in terms of climate change and loss of ecosystems. The biggest driver of deforestation is agriculture. Farmers chop down trees in order to plant crops. Logging operations that provide the world's wood and paper products also cut countless trees each year. Forests are also destroyed as a result of growing urban sprawl, as land is developed for dwellings.[8]

The effects of deforestation are great, but not irreversible. With precise monitoring, we can combat deforestation can help prevent further loss of biodiversity.

Many Earth Observation satellites are orbiting Earth every day and are collecting data that help us monitor changes of land cover in a large scale. This provides a unique opportunity to observe the ever-changing forests and provide regular updates on their conditions at a range of spatial and temporal resolutions.

To get the most out of EO data, many tools of ML and AI as well as geospatial data abstraction libraries are available.

The main goal of the thesis is to identify and apply different techniques for deforestation detection from satellite imagery. Find out what are the advantages and disadvantages of each technique.

The thesis cover principles of radar and multi-spectral data obtained from Sentinel-1 and Sentinel-2 satellites. It shows how to download data, describes data pre-processing, explains the theory behind analytical methods and neural networks. Four different techniques were tried to detect deforestation from satellite imagery. It explains that data availability is not enough. With radar data, the interpretation of the data is as important as access to them. Multi-spectral data on the other hand face the challenge of clouds. The challenge is to extract interpretable information and knowledge from this big data, ideally in almost real-time.

We have conducted experiments with all mentioned techniques for detecting deforestation and compared the results with the Global Forest Change dataset.

Chapter 2

Earth Observation

Earth observation is the gathering of information with remote sensing technologies. Satellites are collecting data about land, oceans, ice, and atmosphere. This is important because we need to understand how the Earth works and to know more about how it's changing.

When it comes to monitoring our planet the great advantage of satellites is that they can cover the entire planet regularly. Earth observation satellites also collect information that is hidden to the naked eye. With remote sensing data, we can make measurements of the Earth's surface on a global scale and also at any specific location in very high resolution.

Multi-spectral remote sensing data are integral, but monitoring forests can be challenging in cloud-prone regions. Radar remote sensing overcomes these challenges because of its ability to penetrate through clouds and scan the surface.

2.1 Copernicus program

Copernicus is the European programme for monitoring the Earth and its environment. It is header by the European Commission in partnership with the European Space Agency.

The Copernicus programme is served by a constellation of satellites - the Sentinels. The satellites and contributing missions generate 12 terabytes of data daily. These satellite data are accessible on a free, full, and open access basis.[3] Data are available back for years, are made comparable and searchable, thus ensuring the monitoring of changes.

2.2 Multi-spectral data

The Sentinel-2 mission consists of a constellation of two satellites. Both are on polar the same sun-synchronous orbit phased at 180 degrees to each other. The satellites scan the land surface conditions with multi-spectral images with wide swath width (290 km) and high revisit time - 2 or 3 days at mid-latitudes under cloud-free conditions.[6]

2.2.1 Bands (Sentinel-2)

Sentinel-2 carries an optical instrument payload that samples 13 spectral bands: four bands at 10m, six bands at 20m, and three bands at 60m spatial resolution.

Multi-spectral data with 13 bands in the visible, near infrared, and short wave infrared part of the spectrum. Figure 2.1 shows different properties of the electromagnetic spectrum.

The spectral bands of Sentinel-2 are listed in the table 2.1. Multi-spectral data are dependent on the weather. The scanned parts of the spectrum do not penetrate clouds.

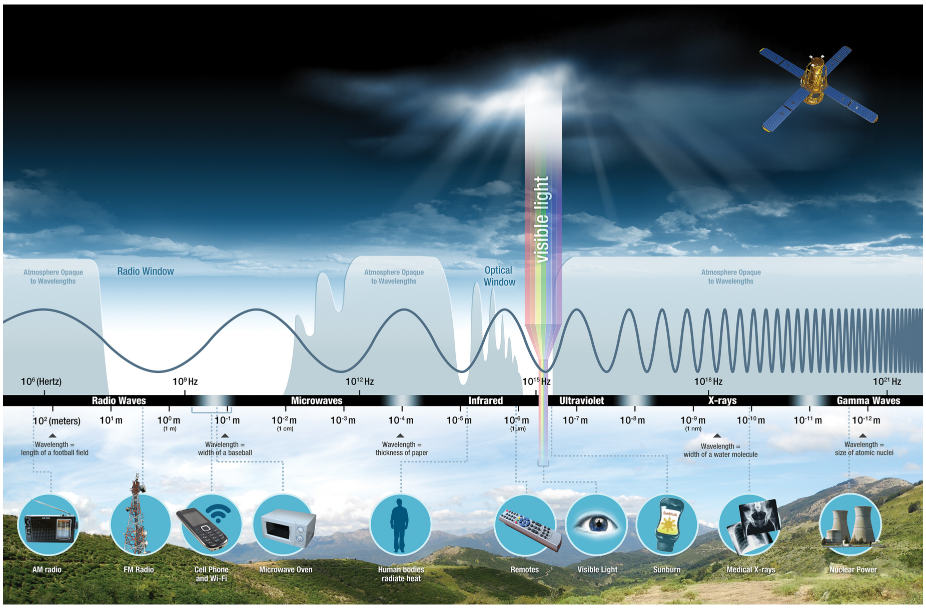

Figure 2.1: The electromagnetic spectrum, Taken from [18]

2.2.2 True color

An image is called a true color when it offers a natural color interpretation. This means that the colors in an image appear to a human observer the same way as if the human to directly observed the object. True color composite uses visible light bands red (B04), green (B03) and blue (B02) in the corresponding red, green and blue color channels, resulting in a natural colored result, that is a good representation of the Earth as humans would see it naturally. The true color images, as in figure2.2 is a widely used for displaying satellite imagery.[4]

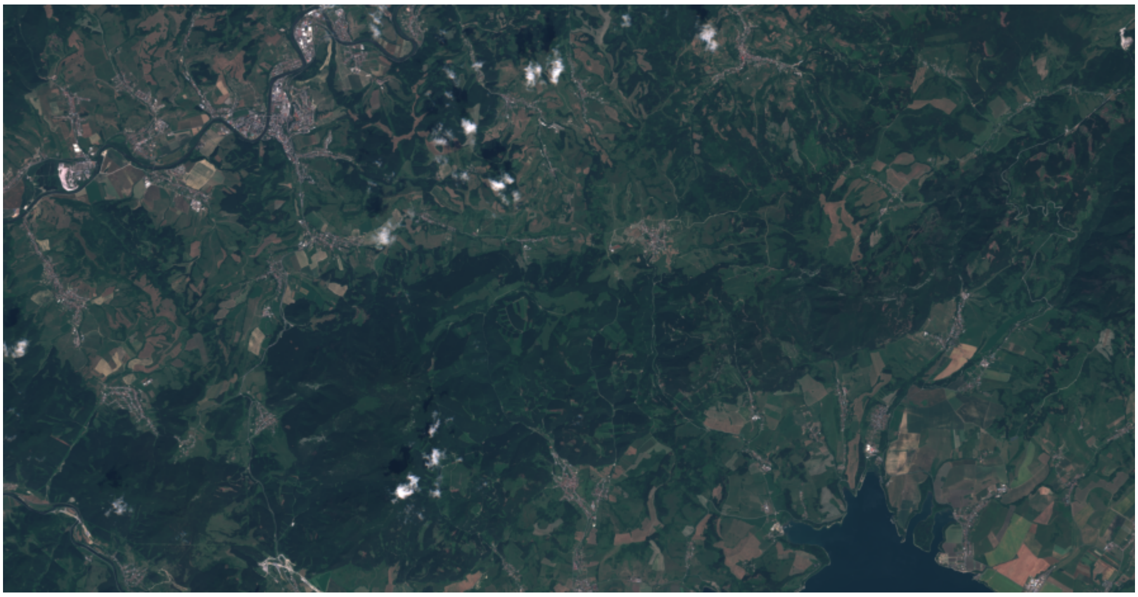

Figure 2.2: True color satellite image. Copernicus Sentinel-2 data.

Name	Description	Resolution
B01	Coastal aerosol	60m
B02	Blue	10m
B03	Green	10m
B04	Red	10m
B05	Vegetation red edge	20m
B06	Vegetation red edge	20m
B07	Vegetation red edge	20m
B08	Near-infrared (NIR)	10m
B09	Narrow NIR	20m
B10	Water vapour	60m
B11	Short-wave infrared (SWIR)	20m
B12	Short-wave infrared (SWIR)	20m

Table 2.1: Sentinel 2 Bands [23]

2.2.3 NDVI

The normalized difference vegetation index (NDVI) is indicator used to monitor vegetation from multi-spectral satellite imagery. It indicates plant's health based on how a plant reflects reflects different light waves.

To understand the state of a plant's health, we need to compare it's absorption and reflection light. The plant leaves reflect green and near-infrared (NIR) waves. The chlorophyll pigment, on the other hand, absorbs red and blue light. Live green plants therefore appear dark in the red spectral range and relatively bright in the near-infrared.[17]

$$NDVI = \frac{NIR - RED}{NIR + RED} \tag{2.1}$$

$$NDVI = \frac{B08 - B04}{B08 + B04} \tag{2.2}$$

NDVI formula exploits these properties. It calculates the ration of difference between NIR and red to a sum of NIR and red, as illustrates equation (2.1). Equation (2.2) shows NDVI calculation from Sentinel-2 bands. The index values range from -1 to 1. NDVI values between -1 to 0 correspond to surfaces like snow, water, sand, stones and infrastructure objects, like roads and houses. NDVI values for plants range from 0 to 1. Figure 2.3 illustrates NDVI visualization.

NDVI is widely used to identify vegetated areas a can be used for deforestation monitoring. The drawback of the NDVI is it's dependence on the weather. Red nor NIR waves can not penetrate the clouds.

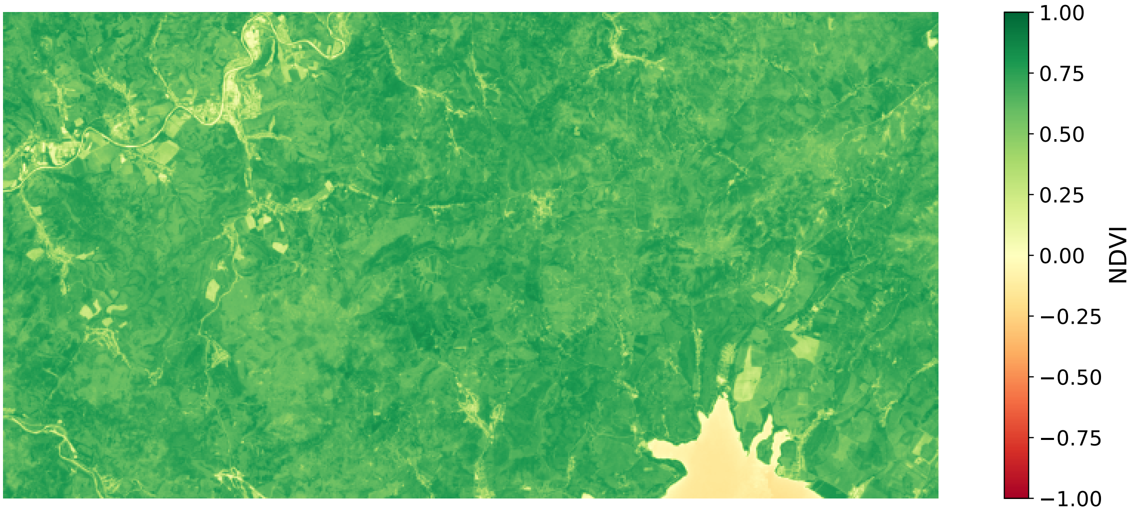

Figure 2.3: NDVI visualization of satellite image. Index was calculated from as mean from all valid (cloudless) pixels from acquisitions between 2019-05-01 and 2019-07-31. Image displays area of Chočské vrchy. The index values are represented with diverging color-map RdYlGn. Values approaching -1 are displayed with red color, values around 0 are yellow and NDVI with values approaching 1 are green. Healthy vegetation is naturally displayed as dark green; water bodies and buildings are yellow. Processed Copernicus Sentinel-2 data.

2.3 Radar

Synthetic aperture radar (SAR) data can be used to monitor changes on Earth surface, including deforestation and it's characteristics allow overcome some of the shortcomings of optical remote sensing. Thanks to independence to solar light and cloud cover all radar acquisitions of the surface produce valid data.

It is a system that actively emits electromagnetic microwaves and receives the backscattered signal from the surface. Radar signal uses frequency, which penetrates through clouds and rain. Therefore the radar technology is independent to solar illumination and weather. Image is reconstructed from the returned pulses reflected by each object. Each pixel represents complex quantity and it's value express intensity of the reflected echo.[5] Example of radar image is shown in figure 2.4.

Unlike most optical imaging systems, which point their sensors towards nadir, the radar antenna is pointed away from nadir by a so-called look angle such that it illuminates a continuous swath on the ground as the aircraft moves along. This results in some unique characteristics such as foreshortening, layover, and radar shadow.

2.3.1 Sentinel-1

Sentinel-1, illustrated in figure 2.5, is operational since 2014 so we have relatively long history of radar data.

Sentinel-1 operates in different modes: Extra Wide Swath – for monitoring oceans and coasts, scans 400km swath width, 20x40m resolution; Strip Mode – by special order only and intended for special needs, scans 80km swath at 5x5m spatial resolution; Wave Mode

Chočské vrchy, SAR

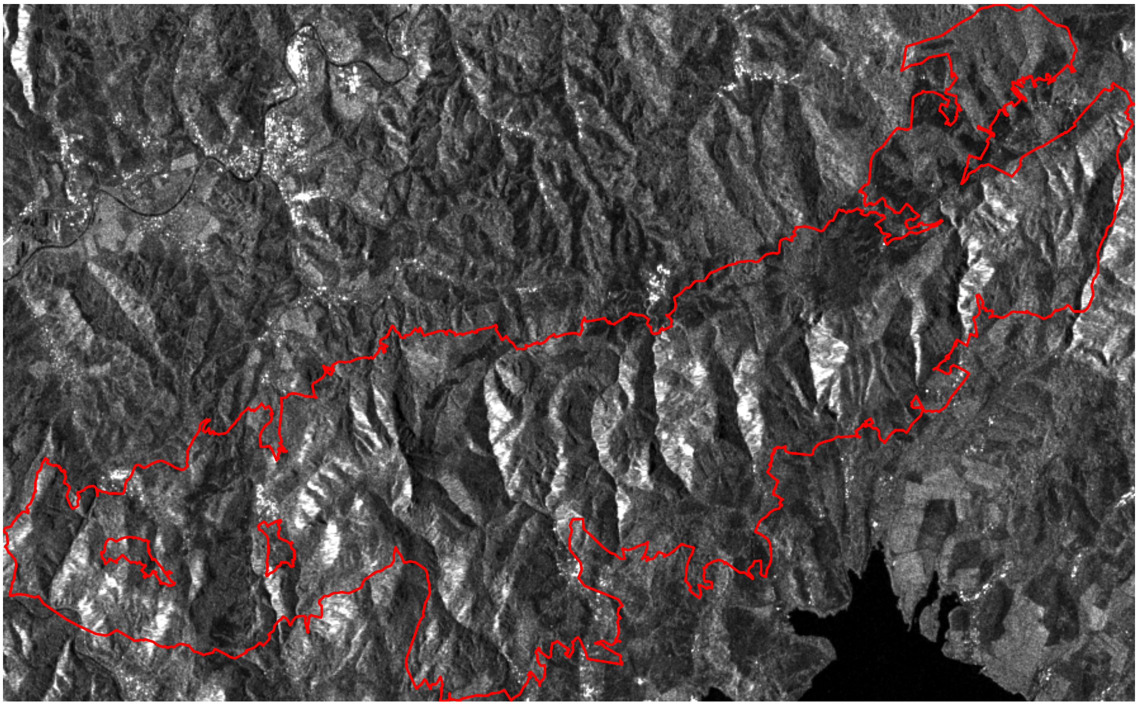

Figure 2.4: Radar image visualization. Processed Copernicus Sentinel-1 data.

– routine collection for the ocean, scans 20km swath with 5x5m resolution; Interferometric Wide Swath – routine collection for land, 250km swath width, 5x20m resolution.

Interferometric Wide Swath is a collection suitable for analysis.

2.3.2 Radar parameters

It's important to understand how radar data can be applied for analyzing.

It is not appropriate to combine SAR imagery from a set of varying sensor parameters if the backscatter data are not carefully cross-calibrated. Combining data from ascending and descending orbit in the analysis will give invalid results.[10]

Radar data are difficult to interpret because multiple parameters influence the resulting image:

- wavelength, polarization, incidence angle, surface moisture, wind
- radar shadow (topography)

There are more radar characteristics than described in this chapter. Speckle effect, dielectric properties, sensor wavelengths, and more have also effect on the accuracy of the analysis. But we cannot influence them or are processed automatically on the provider side. From the practical point of view, it's not significant to pay much attention to them.

Proper selection of the following parameters during pre-processing is required for accurate analysis. Below are described the most important attributes of radar data. Each is explained how affects results and how we should pre-process data to get the best results in analysis.

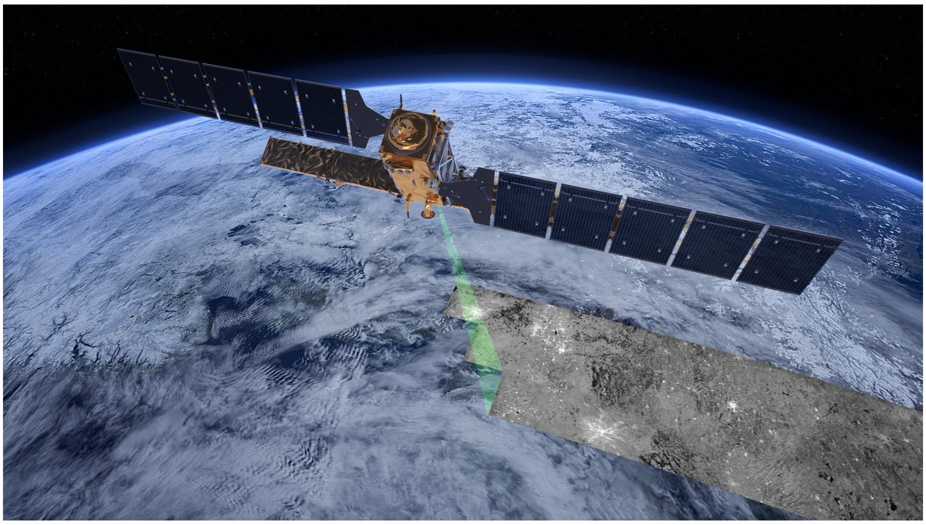

Figure 2.5: Illustration of Sentinel-1 mission, taken from [7]

2.3.3 Polarization

Polarization is orientation of the electromagnetic wave.

The polarization's are usually controlled between horizontal (H) and vertical (V). All combinations are in table 2.2.

Abbreviation	Transmitted signal	Received signal	Type
HH	Horizontal	Horizontal	Co-polarized
HV	Horizontal	Vertical	Cross-polarized
VV	Vertical	Vertical	Co-polarized
VH	Vertical	Horizontal	Cross-polarized

Table 2.2: Radar polarization

Different polarizations can determine the physical properties of the object observed, shown in figure 2.6.

In forested areas, the dominant scattering mechanism is volume scattering. That means that the cross-polarized signals will have a higher return than the co-polarized signals. Thanks to these characteristics are cross-polarized data suitable for detecting forest clear cuts.[10]

2.3.4 Surface topography

Elevation displacement is the image displacement toward the nadir point. Topographic features (mountains, buildings) will be displaced from their desired orthographic position in an image. Geometric distortions caused by side looking properties of the radar, such as layover, foreshortening, and radar shadow, the topography will strongly influence the radar image.

Foreshortening occurs when the hill slopes facing the sensor are mapped as having compressed scale. They appear very bright in the image. It's special case of elevation displacement.[10]

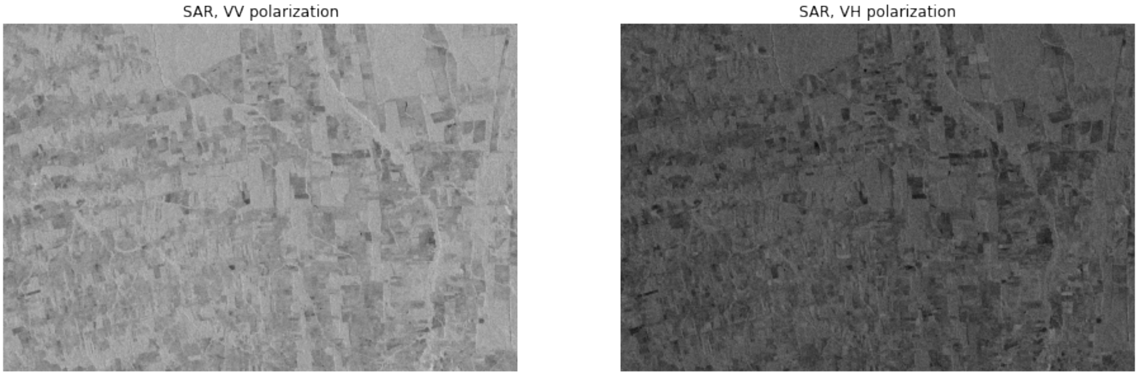

Figure 2.6: Compared co-polarized and cross polarized data. Scene over Rondônia, Brazil. Copernicus Sentinel-1 data 2020.

Layover is an extreme form of elevation displacement in which the top mountain is closer to the radar that are the lower ports. In image the tops of mountains are imaged ahead of their base towards the radar.[10]

Radar Shadow is the absence of radar illumination because of intervening objects. The back-side of the mountains is not visible to the Radar system, hence no information can be collected.[10]

Orthorectification removes terrain distortions from SAR image data using elevation models.

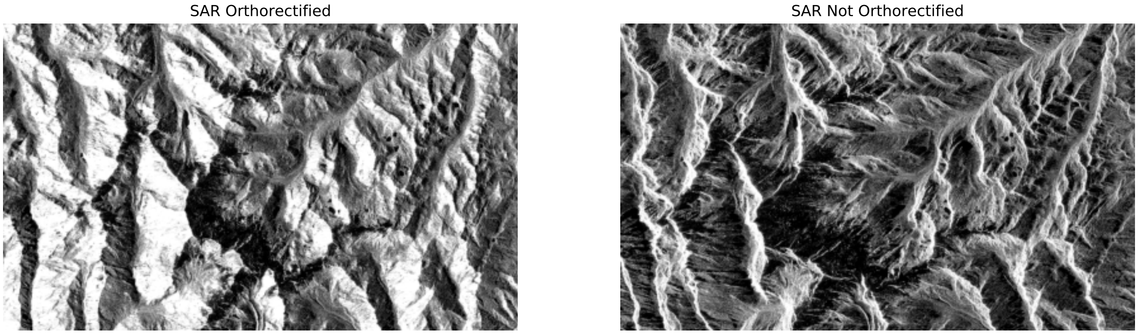

Figure 2.7: Compared orthorectified and not orthorectified data. Copernicus Sentinel-1 data.

Figure 2.7 shows 2 images. On the image on the left the distortions were orthorectificaly corrected. In the image on the right are visible all forms of distortions because of elevation displacement.

2.3.5 Flight direction

SAR satellite is scanning land in two flight orbit directions: ascending and descending. As shows figure 2.8 the data are represented differently. It's caused by different location of the satellite and look angle.

Different look directions have differences in the backscatter and should not be combined in single analysis, otherwise signal variations can be misinterpreted as true change, though no change has actually occurred.

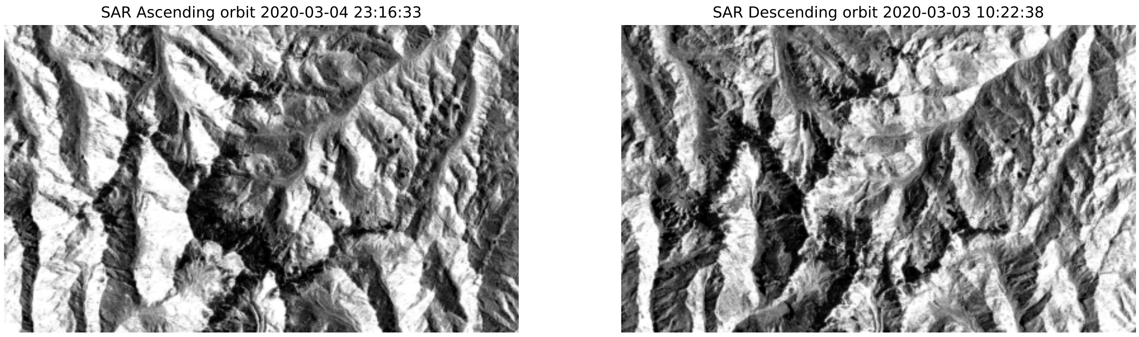
SAR Ascending orbit 2020-03-04 23:16:33
SAR Descending orbit 2020-03-03 10:22:38

Figure 2.8: Compared ascending and descending orbit. Copernicus Sentinel-1 data.

2.3.6 Data Scaling conventions

Different backscatter data scaling are used when storing in different formats. Table 2.3 presents data scaling conventions.

Format	Units	No data value
float32	SAR power data	0
unsigned 16 bit	SAR amplitude data, linearly scaled digital numbers	0
unsigned 8 bit	Decibels (dB) an a logarithmic scale	0

Table 2.3: Radar Data Units

Figure 2.9 shows different distribution of data values in the same image for different scaling. The different distribution of data values can be seen also in visualizations in figure 2.10.

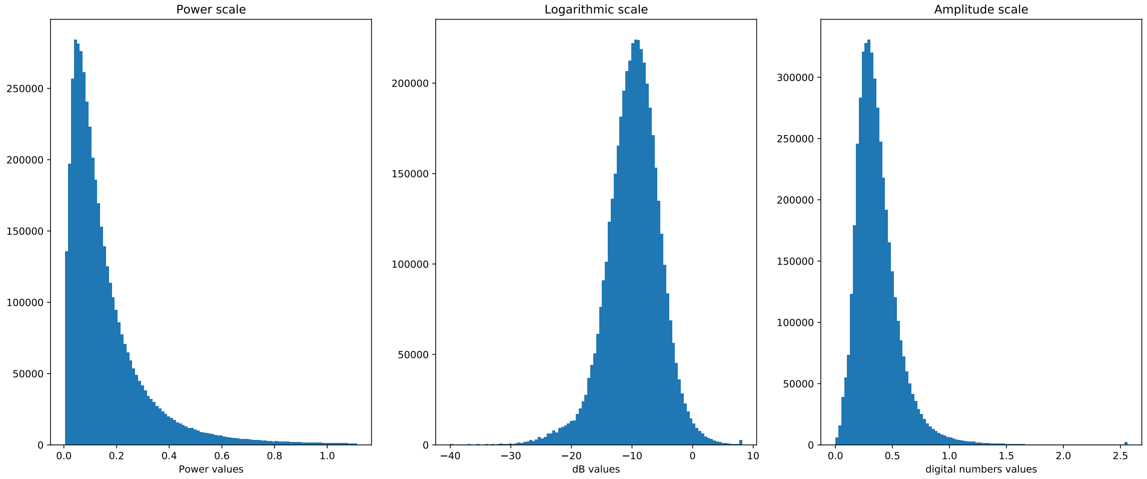

Figure 2.9: Comparison of histograms of SAR Backscatter in different scales

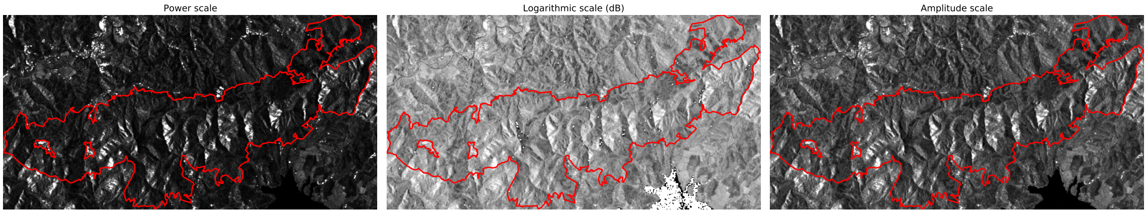

Figure 2.10: Comparison of of SAR images in different scales

With SAR data handling, it is important to perform all operations in the power scale. SAR data expressed in dB or amplitude scale introduce mathematical errors when using these averaging or spatial convolution operations. Therefore, it is advised that data be converted to the power domain during processing.[10]

2.4 Coordinate reference systems

A coordinate reference system (CRS) is a methodology used to specify element in space. There are many different CRS used in practise because each of them better represent some features of the data or optimise for specific region (e.g Europe). Two main types of coordinate systems are Geographic coordinate systems and Projected coordinate systems. Standard Geographic coordinate systems such as World Geodetic System (WGS84 in the latest version) are best for global analysis with downside of distorted distance using latitude and longitude. Commonly used Projected coordinate systems is Universal Transverse Mercator (UTM) which divides globe into zones and regions and use regional projections and coordinate system grid is projected using the Mercator projection. UTM system is better to be used for doing analysis in specific region since it is more accurate in representing distance and area.[15]

2.5 Neural Networks

It is widely known, that neural networks(NNs) or artificial neural networks(ANNs) in computer science, came from imitation of biological neural networks and the brain's ability to learn. When we look at the schemas of neural networks it is a collection of several nodes also called neurons and many connections between them. Neuron itself is a mathematical function with several inputs and a single output. Connections between these nodes have weights that express the kind of strength between the nodes. All these weights are important mainly because they can tell the neuron to respond more to some inputs than others. Firstly, we can assign weights to connections randomly. When we start to insert inputs into a neural network, the result will look pretty random as well. So we need to traverse network backward from the output to the input and change the weights. After many, usually hundreds of thousands of cycles, we can hope that all the weights will be corrected and results will be satisfying. In computer science, we call this approach Backpropagation and it simply represents a method that is able to backpropagate an error. Today we use neural networks for several different use cases as for example:

- Object identification of images and videos
- Speech recognition

- Image processing
- Machine translation

Today widely used architectures are:

- Perceptron
- Convolutional Network
- Recurrent Networks
- Autoencoders

2.6 Unet architecture

U-net architecture is widely used Convolutional neural network architecture which builds upon the concept of Fully Convolutional network. The main difference is replacing pooling operators in the successive layers with the upsampling operators to increase resolution of the output. High resolution features are combined with upsampled output in order to localize. The network architecture consists of two parts and 23 convolutional layers in total. First part (left side in the Figure2.11) has a typical architecture of convolutional neural network consisting of repeated application of 3x3 convolutions without the padding. Rectified linear unit (ReLU) is used as an activation function and 2x2 max pooling operation with stride 2 is used for downsampling. Feature channels are doubled at each downsampling step. Second part (right side in the Figure Figure2.11)) consists of upsampling feature map followed by 2x2 convolution that reduces number of feature channels and concatenate the correspondingly cropped feature map from the first part. ReLU is used as an activation function also for this part. Final layer has 1x1 convolution used to map each 64-component feature vector to the desired number of classes. The input image size should have even width and height so 2x2 max-pooling operations can be applied to a layer.[20]

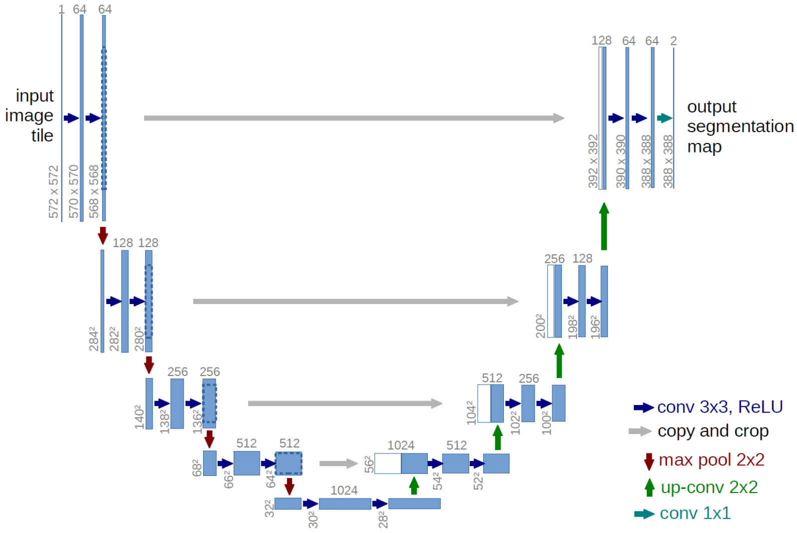

Figure 2.11: Original U-Net architecture, taken from [20]

2.7 Global Forest Change dataset

Global Forest Change is dataset containing analysis characterizing global forest extent and change from 2000 through 2018. This global dataset is divided into 10x10 degree tiles, consisting of seven files per tile. All files contain unsigned 8-bit values and have a spatial resolution of 1 arc-second per pixel, or approximately 30 meters per pixel at the equator. In the dataset is mapped global tree cover extent, loss, and gain for the period from 2000 to 2012 at a spatial resolution of 30 m, with loss allocated annually.

`lossyear` data represents forest loss during the period 2000–2018. Events where change from a forest to non-forest state are included. Foress loss is encoded as either 0 (no loss) or else a value in the range 1–17, representing loss detected primarily in the year 2001–2018, respectively.[13]

Chapter 3

Solution proposal

3.1 The main objective

The main goal of the thesis is to identify and apply different techniques for deforestation detection from satellite imagery. Find out what are the advantages and disadvantages of each technique: It can be about the complexity of the calculations when it takes several minutes to perform the calculations; Demand for resources where neural networks need a powerful graphics card, and a lot of time to train; Accuracy of results and others.

To successfully run any of the analyses, it is necessary to download and pre-process the satellite data. It is necessary to select the provider data appropriately. A good data provider can save a lot of time, otherwise spend on regular data pre-processing.

3.2 Architecture

Figure 3.1 displays the proposed workflow of data analysis with different techniques. It starts with properly selecting the study area. The study area should have some structured data representation, ideally in format with geospatial information so the boundaries of the area can be exactly determined.

We download the satellite imagery and dataset with ground truth within the boundaries of the specified study area. The neural network for image segmentation needs to input true color images. One analysis detects changes in NDVI index. Both true color and NDVI representations are created from multi-spectral satellite imagery. Other techniques work with radar date from a different satellite.

Each technique needs different data preparation for the analyses to be performed. The neural network expects on the input cloudless images with labels of deforested patches. Information about forest loss will be extracted from a suitable dataset. Analysis that detects changes in NDVI needs mean values from multiple satellite acquisitions calculated from cloudless data. Techniques analyzing radar data works only if the data are in the correct scale.

The output from all techniques will be in the same format. This ensures that results can be compared to each other and with ground truth dataset.

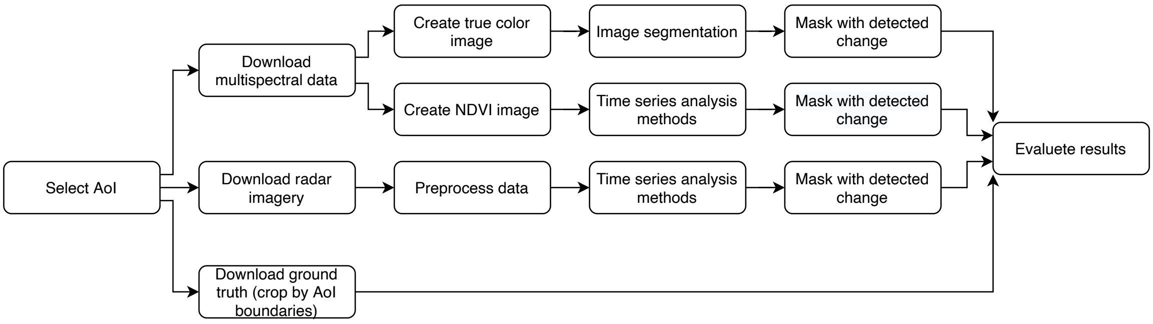
Create true color image
Image segmentation
Mask with detected change
Download multispectral data
Create NDVI image
Time series analysis methods
Mask with detected change
Evaluete results
Select AoI
Download radar imagery
Preprocess data
Time series analysis methods
Mask with detected change
Download ground truth (crop by AoI boundaries)

Figure 3.1: Proposed architecture

Chapter 4

Implementation of techniques for deforestation detection

4.1 Tools and formats used in analysis

This section describes the main tools for processing geospatial data. The list contains tools used for downloading, transforming, executing mathematical functions data, as well as tools for performing analysis and training neural networks. The most common geospatial formats for storing data are also described.

4.1.1 Data Analysis tools

Python is an increasingly popular tool for data analysis. The following paragraphs introduce libraries and tools used in the thesis for performing data analysis.

NumPy is the package for scientific computing in Python. It supports multidimensional arrays and contains a collection of mathematical functions to perform on these arrays.[2]

Shapely is a BSD-licensed Python package for manipulation and analysis of planar geometric objects. Shapely is a Python package for analysis and manipulation of planar objects, where objects represents geometries such as point, polygon, line or their collection. Data are not represented in any specific format or coordinate system, but can be extended with packages uses this information.[21]

GeoPandas is built on top of Pandas and NumPy libraries and can easily facilitate dealing with Geographic Data. GeoPandas provides not only the capability to read and manipulate geographic data easily but also can perform many essential geospatial operations including among others geometric operations and projections which it borrows from the Shapely library. Together with shape information, it stores its coordinate reference system as an attribute on an object. Objects may be transformed to new coordinate systems.[12]

GDAL is a collection of software that helps with the translation of data from different file formats, data types, and map projections.[11]

Rasterio is a Python geospatial library that wraps the features of the GDAL in Python functions and classes. It reads and writes data files in GeoTIFF image format to store georeferenced raster datasets such as satellite imagery. Rasterio provides a Python API based on NumPy arrays and GeoJSON.[16]

eo-learn is an open-source Python library. It has a modular design of packages for the extraction of information from satellite imagery. eo-learn contains modules for typical Earth Observation value extraction tasks, such as data downloading, cloud masking, or

NDVI computation. The library uses NumPy arrays and Shapely geometries to store and handle satellite data.[22]

The sentinelhub Python package allows downloading and processing of satellite images. It primarily supports Sentinel Hub Services, however, it also provides data from other sources and has a wide range of useful utilities. It supports the downloading of Sentinel-1 and Sentinel-2 imagery among other sources.[24]

The fastai high-level library simplifies training fast and accurate neural nets using modern best practices. It is built on top of the PyTorch framework. The vision module of the fastai library contains all the necessary functions to define a dataset and train a model for computer vision tasks.[9]

4.1.2 Analysis formats

Most of the geospatial data are stored in two formats. GeoJSON for text data structures and GeoTIFF for georeferenced images.

GeoJSON is a open standard format for encoding a variety of geographic data structures such us polygons, points, and lines. It is based on JSON GeoJSON files are stored with standard extension .json or .geojson. [14]

GeoTIFF is standard which allows georeferencing information to be embedded within the image file. The georeferencing information contains spatial information about the image file such as map projection, coordinate systems, ellipsoids, or dates.[19]

4.2 Study area

Selecting a suitable study area is needed for selecting a subset from large geospatial data. The data can analysis-ready dataset or satellite imagery. In technical studies or code examples, the study area is referred to as an area of interest (AoI). With AoI in a proper format, it can be used for cropping downloaded, or specifying boundaries of yet to download data.

4.2.1 Chočské vrchy

Chočské vrchy area was chosen as a study area. It is located in the in north-central part of Slovakia, covering a total area of 16817,5 Ha. The area is mountainous with the highest peak Veľký Choč 1611 meters above sea level. The forest cover is mainly represented by coniferous trees. Foothill meadows, pastures, and fields are on the edge of the deforested areas [1]. The view from satellite is displayed in 4.1.

The site is listed in a network of threatened and important areas known as Natura 2000. The initiative Natura 2000 aims at assuring the protection of the most valuable and endangered ecosystems in support of EU policies. The geospatial data of all Natura 2000 sites are accessible from the European Environment Agency datasets portal [1].

4.2.2 Boundary for data download

Before downloading satellite data, it is necessary to specify the bounding box of the area for which we want to download images. Geospatial tools can calculate bounding box from areas displayed in GeoTIFF images or polygons saved in GeoJSON files.

[1] https://www.eea.europa.eu/data-and-maps/data/natura-11/natura-2000-spatial-data

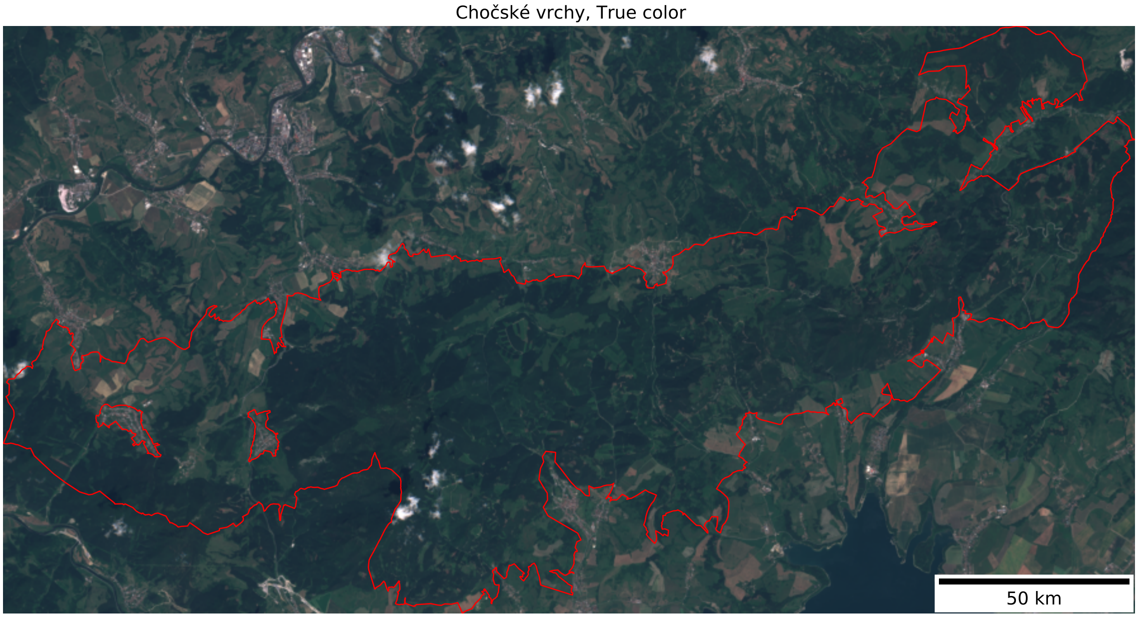

Figure 4.1: Chočské vrchy, Slovakia is the geographic location of the study. Red line represents the boundary of Natura 2000 site SKCHVU050. Basemap: Sentinel 2 true color image.

Before further processing, it is necessary to check the projection in which the data is stored. The satellite data we download will be with the same projection as the bounding box. As mentioned in section 2.4, the most suitable projection for analysis is the UTM because it minimizes distortions within the zone. For our study area the ideal projection is UTM zone 34N: EPSG:32634.

4.3 Analytical methods for deforestation detection using radar data

4.3.1 Preparing dataset for analysis

Analytical methods for deforestation detection works with SAR data. In this analysis, data from Sentinel-1 are used. `WcsRequest` handles data download. It important to specify on the format of the data. Data in power scale are required to perform analysis. This is ensured when the data type is `FLOAT32`. More info for data types is in section 2.3.6.

`WcsRequest` also returns acquisitions, which only partially scanner the area in the bounding box. All non complete data are filtered out by checking `dataMask` flag. The valid data are saved to disk in `GeoTIFF` format.

The saved images contains 2 channels: one for data band and the other is `dataMask` flag. With tool `gdal_translate` all images are converted and have only one band. This step is important, because `gdalbuildvrt` cannot build dataset from multidimensional images.

`gdalbuildvrt` takes all downloaded images and creates virtual GDAL dataset. The dataset only contains links to original files. This dataset can be loaded with `GDAL` Python library and read as NumPy array. The shape of `NumPy` array is `(89, 1542, 2968)`. That means 89 images with dimensions 1542x2968px are loaded.

4.3.2 Computation of time series metrics

Since we have data in power scale, they can be used in calculations. Only invalid values needs to be skipped in computation. When data are in `FLOAT32`, the invalid values are 0. With series of `NumPy` computations, we can replace them with `np.nan` values. The `NumPy` is able to skip `np.nan` values in other computations.

4.3.3 Change detection with the Coefficient of Variation Method

Three metrics for each pixel in the stack need to be computed for this method: `mean`, `variance`, and `coefficient of variation`. `Mean` and `variance` are calculated with built-in `NumPy` functions, `coefficient of variation` is then calculated as the ratio of the `mean` and the `variance` as shown in equation 4.1

$$cp_{x,y} = \frac{\sigma^2_{xy}}{\bar{x}_{xy}} > t \tag{4.1}$$

Figure 4.2 show frequency of changes calculated with coefficient of variation with selected threshold for classifier.

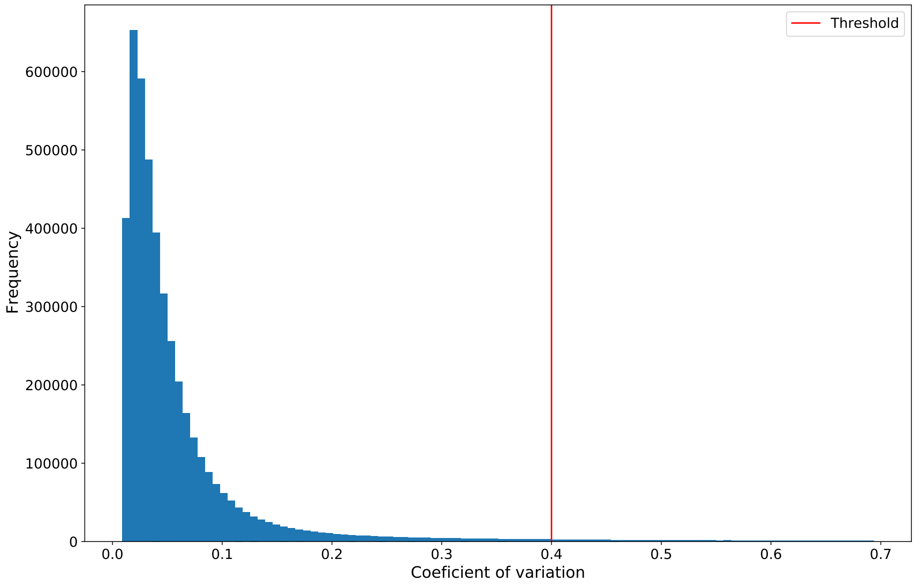

Figure 4.2: Histogram of coefficient of variation

Detected changes are displayed in figure 4.3.

4.3.4 Change detection with Percentile Difference Threshold Method

Change detection with Percentile Difference Threshold Method is based on applying threshold on the 95th and 5th percentile difference, see equation 4.2. The advantage to look at percentiles versus maximum minus minimum is that outliers and extremes in the time series are not influencing the result.

$$cp_{xy} = P^{95th}_{xy} - P^{5th}_{xxy} > t \tag{4.2}$$

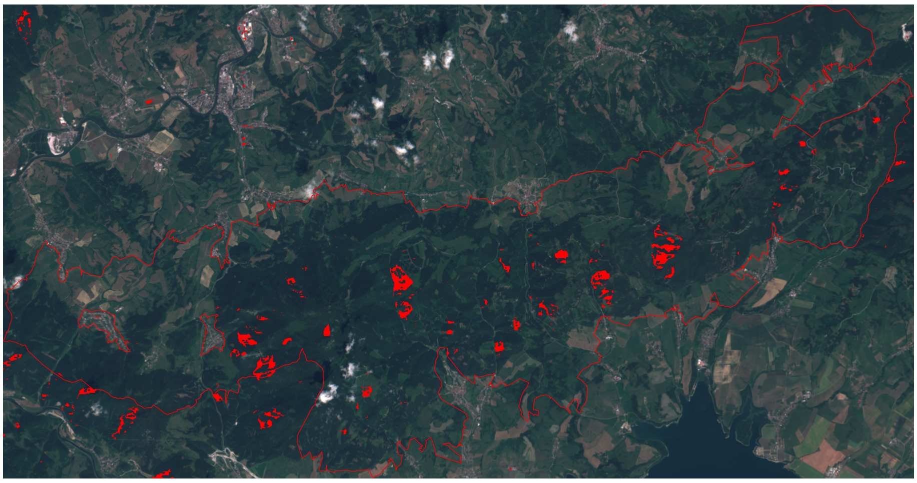

Figure 4.3: Detected changes using SAR coefficient of variation classifier showed over true color image

Figure 4.4 show frequency of changes calculated with percentile difference threshold method with selected threshold for classifier.

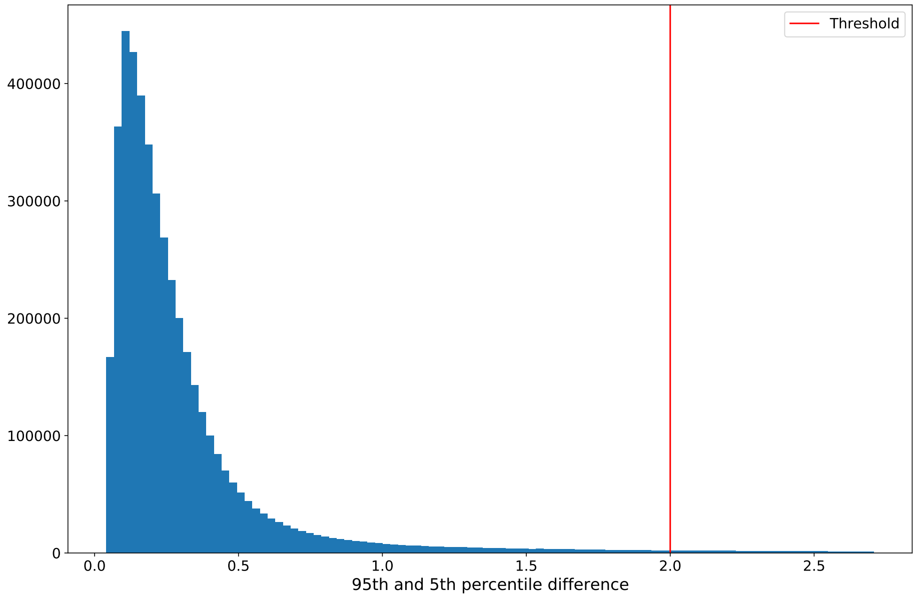

Figure 4.4: Histogram of percentile difference

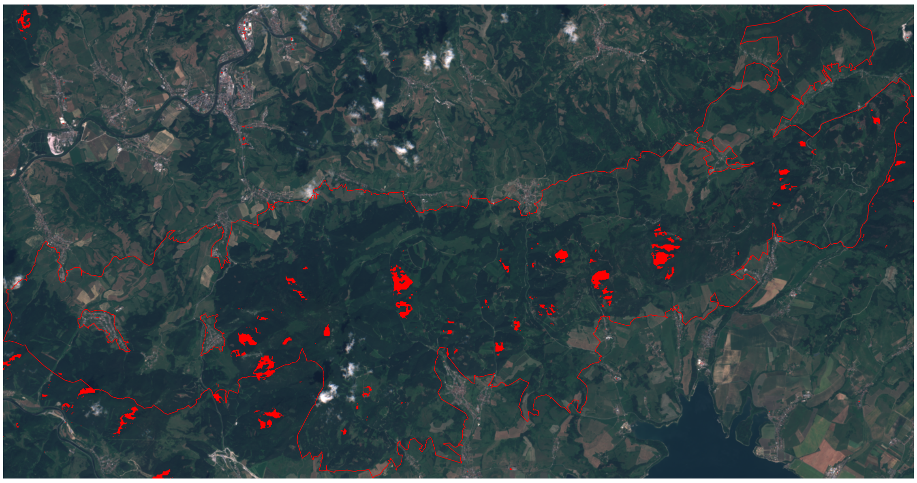

Figure 4.5: Detected changes using SAR Percentile Difference Threshold showed over true color image

4.4 NDVI based change detection

We will use modules from the `eo-learn` collection to download data and preprocessing. Data download, cloud detection, NDVI calculation and saving data to disk are tasks in single `eo-learn LinearWorkflow`. A workflow is a directed graph composed of instances of `EOTask` objects.

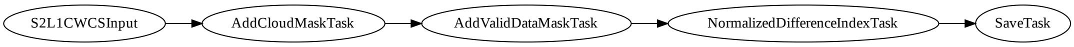

Figure 4.6: eo-learn workflow dependency graph. Workflow contains all tasks that will be executed.

`S2L1CWCSInput` task obtains data from Sentinel Hub services. We specify which Sentinel-2 bands to download. For „NDVI diff“ analysis the bands B04 and B08 are sufficient, another bands B02 and B03 are used for creating true color images. Maximum accepted cloud coverage of an image is set to 50%. It's not problem if part of the area is under the clouds. The next task in workflow detects clouds and only valid data will be used for analysis.

`S2PixelCloudDetector` automatically detects clouds in Sentinel-2 imagery. Detected clouds are added as a mask feature to the downloaded data. `AddCloudMaskTask` task then add cloud mask to downloaded data.

Because satellites scan the ground in narrow parts, called swaths, it can happen that only part of the area in the bounding box will have data. For each pixel, we have `IS_DATA` metadata flag that indicates whether area under the pixel was captured or not. We use this information together with the cloud mask in `AddValidDataMaskTask` to validate pixels with new flag `IS_VALID`.

`NormalizedDifferenceIndexTask` calculates a NDVI from two bands B04 and B08.

`SaveTask` stores Sentinel-2 bands data, cloud masks and other features as `NumPy` arrays to disk.

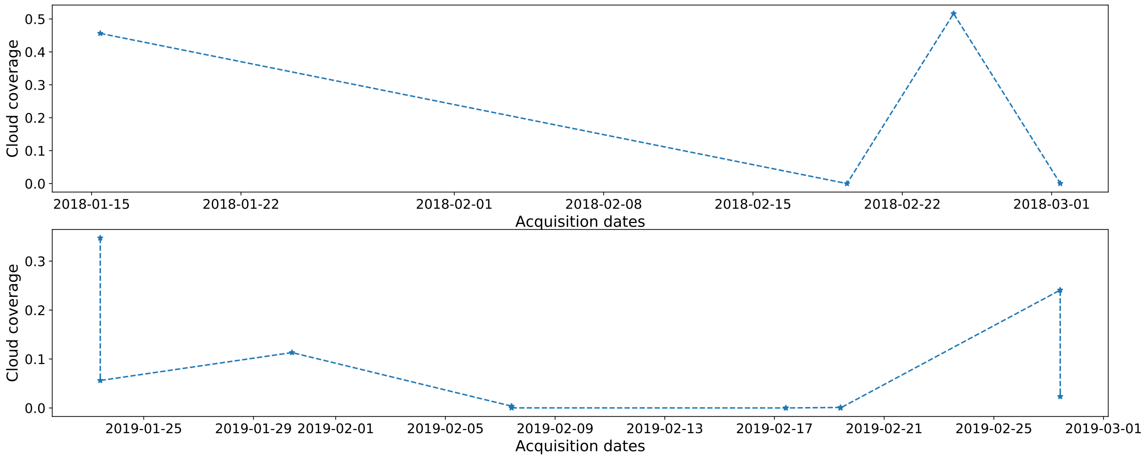

Figure 4.7: Cloud coverage of downloaded satellite data.

The workflow is executed twice. First with date range from 2018-01-01 to 2018-03-01 and next with the same dates in 2019 (2019-01-01 - 2019-03-01). 4 image acquisitions in 2018 and 11 in 2019 meet the conditions specified in input task. Their cloud coverage is shown in figure 4.7.

Further data processing is outside `eo-learn` workflow. Invalid data needs to be filtered out and mean values of NDVI calculated.

The cloud coverage differs across acquisitions. Pixel values on the positions where flag `IS_VALID` indicates that data are missing or area is under clouds are updated to value `numpy.nan`. This ensures, that only valid data will be included in analysis. We can see valid date in the figure 4.8. This specific acquisition was chosen because of high cloud coverage to illustrate cloud data filtering.

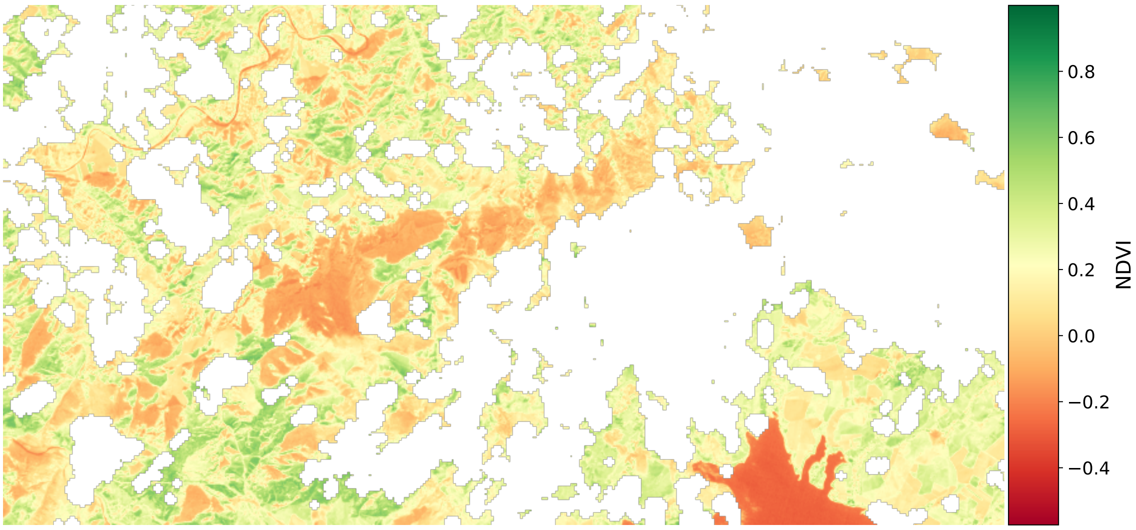

Figure 4.8: NDVI visualization of satellite image with applied `IS_VALID` mask. Clouds cover 45% of the area. Sentinel data acquired 2018-01-15.

The mean value of NDVI is calculated for whole time period in each year, see figure 4.9

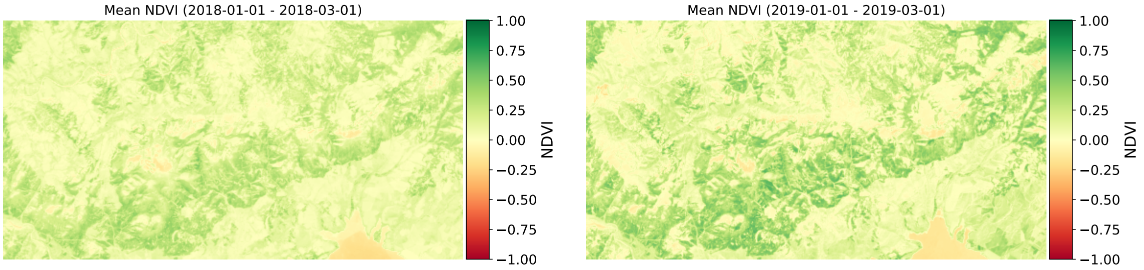
Mean NDVI (2018-01-01 - 2018-03-01)
Mean NDVI (2019-01-01 - 2019-03-01)
NDVI
1.00
0.75
0.50
0.25
0.00
−0.25
−0.50
−0.75
−1.00

Figure 4.9: Calculated mean NDVI for 2018 and 2019. Processed Sentinel data.

For detecting changes, which occurred in 2018, we subtract mean values of 2019 and 2018 and apply thresholds on the results.

The resulted data are displayed in histogram (figure 4.10). From the histogram we choose two thresholds. One for changes where NDVI increased between the years. These changes indicates vegetation growth. The other threshold is for decreased NDVI, or vegetation loss.

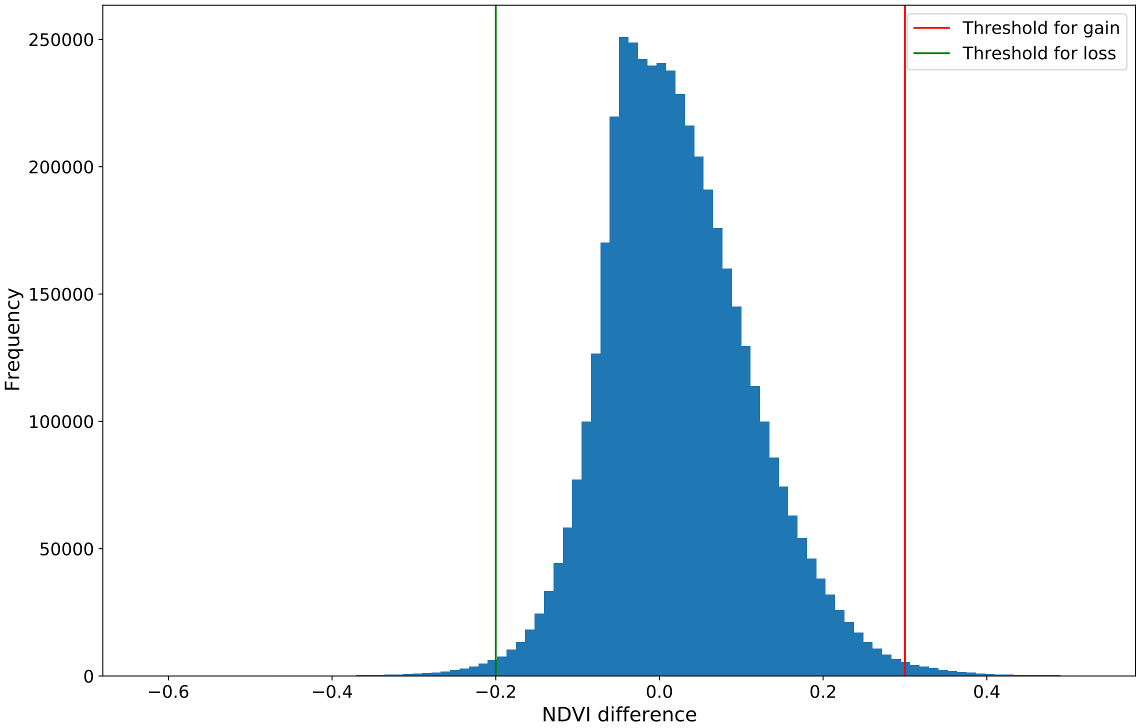

Figure 4.10: Histogram of NDVI change between 2018 and 2019 with chosen thresholds for detecting changes.

The advantage of this method is that it is possible to monitor not only the forest loss but also the growth of new trees. It is computationally undemanding, we do not need a lot of input data and the NDVI also shows other information such as forest health.

The problem with this approach is that we need mean data values from multiple scans or a cloudless image in order to detect changes. It is not possible to say exactly when the change on the earth's surface occurred.

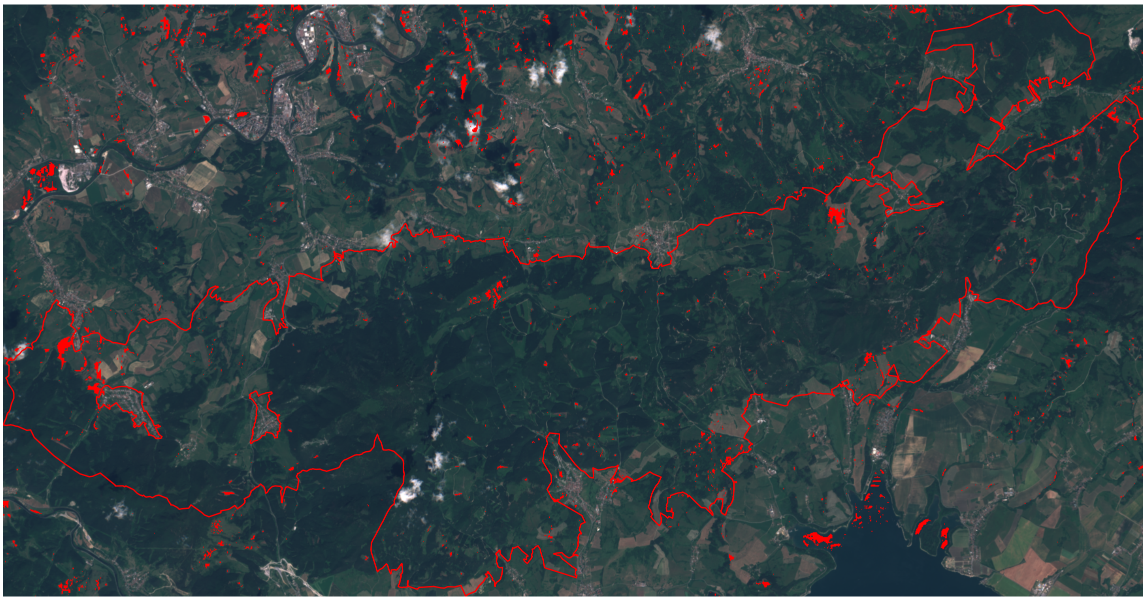

Figure 4.11: Detected changes using NDVI difference displayed on top of the true color image.

It is also necessary to distinguish whether the detected changes occurred in the forest or in the fields. In order to exclude monitoring by detecting events other than deforestation, the result should be combined with, for example, land cover data.

4.5 Detection of deforested patches with image segmentation

4.5.1 Dataset preparation

The neural network predictions are only as good as the data it's trained on. If we have an unbalanced dataset, insufficient quality of data, incorrectly labeled dataset or any other problem in the training data the neural network will not predict valid data. Therefore a well prepared dataset is a very important step in a training neural network workflow.

Neural network will be trained on true color satellite image data with labels created from Global Forest Change dataset described in section 2.7.

`eo-learn` `LinearWorkflow` is again used for downloading data. Workflow is build from tasks for downloading data, detecting clouds, calculating valid data in the acquired image and saving data to disk. Figure 4.12 shows all tasks.

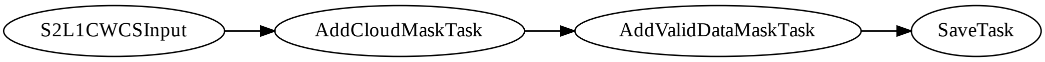

Figure 4.12: eo-learn LinearWorkflow for downloading and pre-processing of Sentinel-2 data.

`S2L1CWCSInput` is again used for obtaining data. For true color images, we need Sentinel-2 bands B02 B03, B04. Training dataset should contain only images without clouds, so maximum cloud coverage is set to 20%. Because we didn't filter out all images which are partly covered with clouds, we use `S2PixelCloudDetector` for detecting pixels with cloud cover. `AddCloudMaskTask` uses the output from the detector for adding a cloud mask to downloaded data. The same as in the NDVI analysis, `AddValidDataMaskTask` computes a new `IS_VALID` flag from the cloud mask and `IS_DATA` flag.

The Unet neural network is expecting on the input images with resolution 256x256px. To achieve this, we can either crop one large image into smaller ones with the desired size, or the bounding box for downloading data will be in a given resolution. `UtmZoneSplitter` takes any arbitrary shape with specified projection and bounding box size to create list bounding boxes. The area of Chočské vrchy is split into 47 bounding boxes with size 2560x2560meters. With resolution 10 meter squared per pixel, this results in images with resolution 256x256px. Figure 4.13 shows the example of such an image.

The time interval for downloading images is from 2018-06-01 to 2019-06-30.

For each downloaded image, we need to add labels, which indicate on which areas the forests were cut. Global Forest Change dataset contains information about forest loss stored in the `GeoTIFF` image. The image of our study area has a different resolution than the downloaded images and can not be simply cropped into the desired size. Because it is georeferenced, the data can be transformed between vector and raster formats.

`rasterio.features.shapes` extract information into vector data - polygons and store them in `GeoDataFrame`.

`VectorToRaster` transforms and crop by `EOPatch` bounding box vector data from `GeoDataFrame` back into a raster feature with the same resolution as downloaded satellite data. Forest loss label for the same area as in satellite image is in figure 4.13

The next step in preparing the dataset is to store downloaded data and their labels as images with names that can be easily referenced. Parts of the downloaded data with

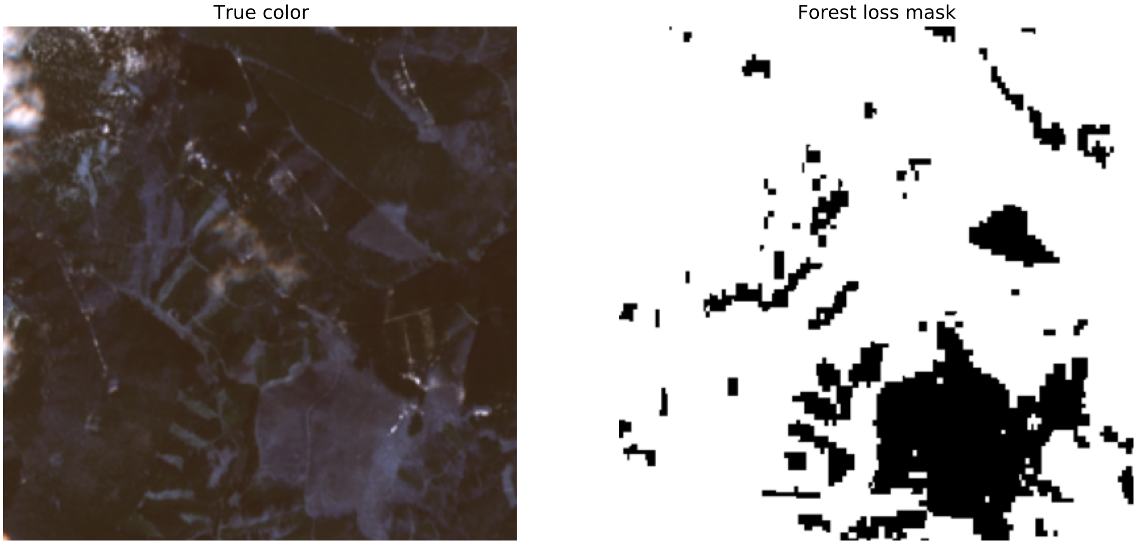

Figure 4.13: Example of image and label in training dataset for image segmentation.

eo-learn workflow can still contain invalid data or be covered with clouds. These images will be filtered out before saving them. 1263 images meet the requirements. But 849 of these images contain no deforested patches in the label. If these images would not be also filtered out, the dataset would be unbalanced. When images, where deforested patches cover less than 10% area are also removed, the final count for training and validation dataset is 414 images.

True color satellite images and images that contain forest loss masks are saved into different folders with the corresponding names. `glob.glob` returns a list of files for each folder. From these lists is generated a `JSON` file, that can be loaded into a `fastai` helper function that loads dataset.

4.5.2 Creating Unet model

`fastai` has module `unet_learner` for loading pre-trained models suitable for transfer learning. `unet_learner` takes several arguments. The most important are `data` where the dataset in a suitable format is loaded for training and validation and `arch` with which the architecture of the pre-trained model is specified.

Dataset needs to be converted info subclass of `ImageDataBunch`. For image segmentation, we use the `SegmentationItemList` class. It has a shortcut for loading image files from `DataFrame` with a column of filenames and a column of labels. The dataset is split into training and validation by a random percentage. Image transformations such as horizontal and vertical flip, rotation, change of lightning for data augmentation are also applied. `fastai` learner uses these transformations during training. Data batch size is specified to 8 images and all data are normalized by ImageNet statistics to match our images with images used to train core architecture. This object can be passed to `unet_learner`.

4.5.3 Fine tuning model

`ResNet34` trained on ImageNet is used as the backbone architecture for the new Unet model. Pixel accuracy is a metric for determining whether the network is training well.

For training our model we need to find a stable learning rate. We use `learn.lr_find()` to pick a good learning rate. Figure 4.14 shows the graph. In the graph, we find some learning rate with a steep slope.

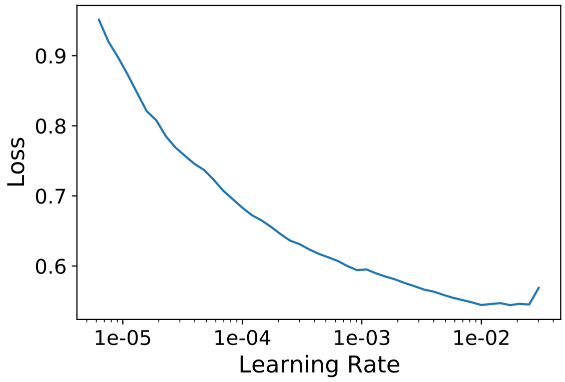

Figure 4.14: Finding learning rate in created Unet model.

Learning rate 1e-03 is chosen from the plot. The model trains with one cycle of 3 epochs. Figure 4.15 shows that training loss is greater than validation loss. This means we are underfitting. We can solve this by training longer.

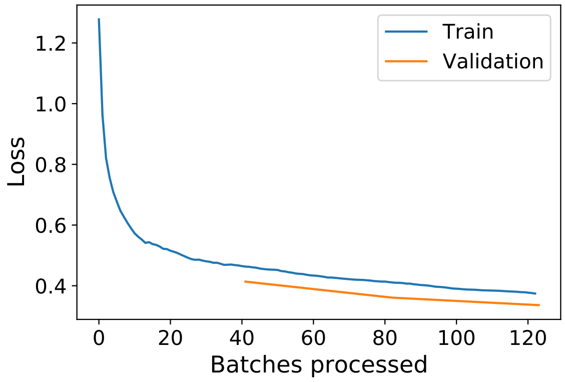

Figure 4.15: Training and validation loss during first stage of training.

The pixel accuracy after the first stage of training is around 28%, but figure 4.16 shows that model already learned to recognize features in the new dataset.

In the next stage of training, we unfreeze the layers of the backbone and fine-tune the whole models. Learning rates are again determined from the graph of `learn.lr_find()`.

The model is trained 2 more times with a frozen backbone repeating the same steps as in the first stage of training. In the forth stage the validation loss was greater than training loss (figure 4.17).

4.5.4 Model results

The results after final stage of training are shown in figure 4.18. In the central part of the example image the model was able to dected deforested patch that was not included in ground truth dataset.

Figure 4.19 shows confusion matrix of the model performance after training.

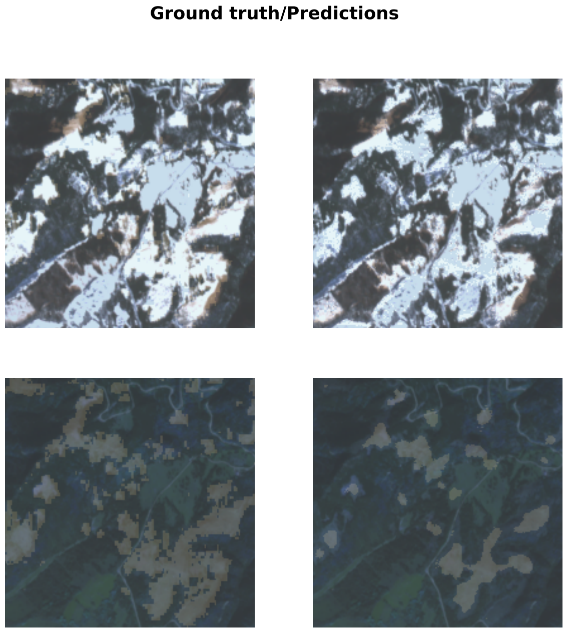

Figure 4.16: Model results after first stage of training.

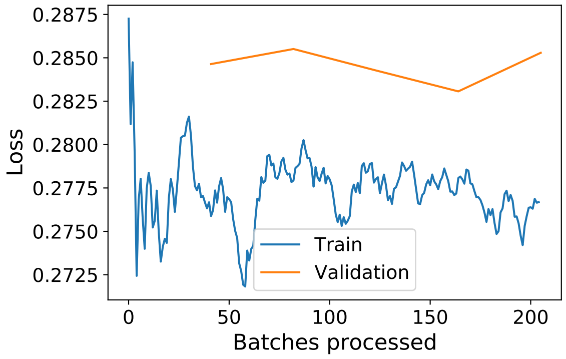

Figure 4.17: Training and validation loss during first stage of training.

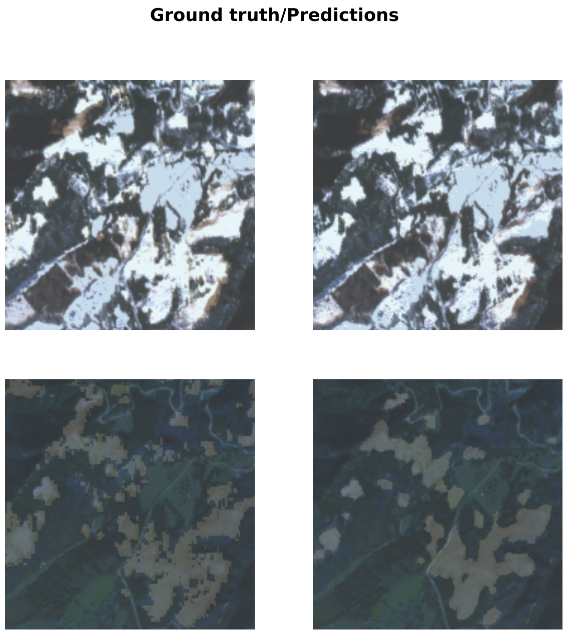

Figure 4.18: Model results after last stage of training.

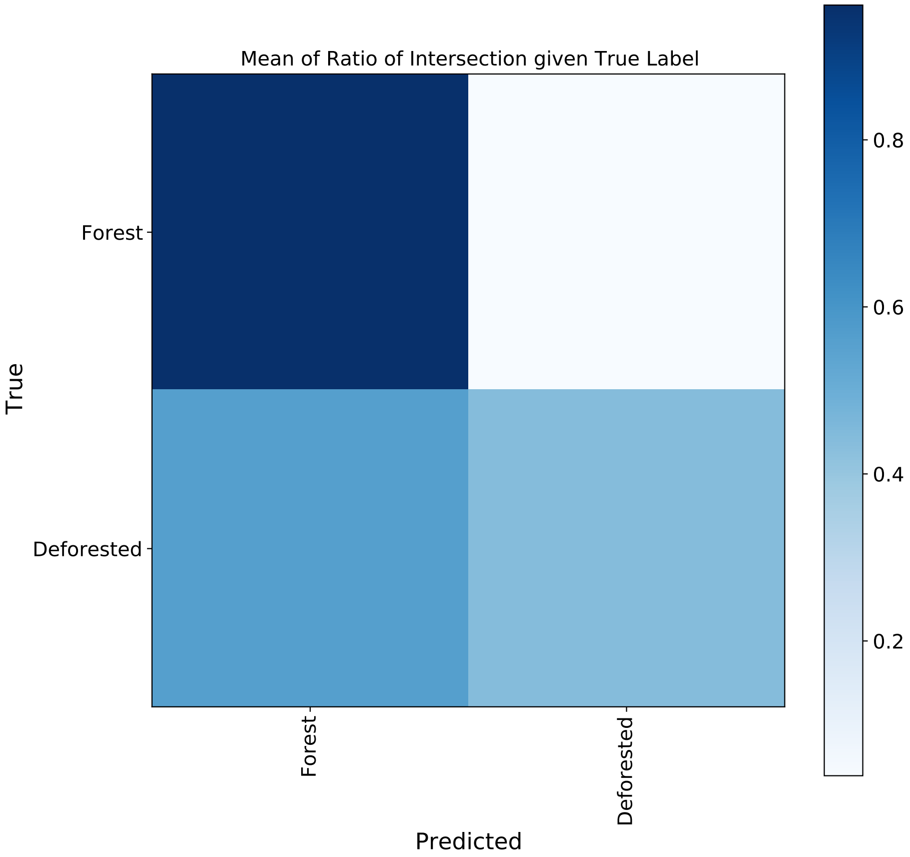

Figure 4.19: Confusion matrix of Unet model performance

Chapter 5

Discussion

All chosen techniques for deforestation detection have been described, performed, evaluated. But there is still a lot of room for improvement. Here are some of the ideas for future development.

- Many of the method's parameters were selected according to values in histogram graphs. Properly evaluating results of analytical methods is needed better methodology than selection according to the author's best knowledge. Metric such as intersection over union should be used for fine-tuning thresholds and other parameters.

- The training dataset for image segmentation contains only 414 images from the same area. For a neural network to generalize better bigger dataset is needed with images from different areas.

- Unet model for image segmentation uses true color images composed of three bands. Some information is hidden in this part of the electromagnetic spectrum but available in other bands that can be used for training. Neural networks are capable of using multi-dimensional data.

- The neural network uses labels for training from the dataset, which is itself the output of some model. Any error in results from the original model is transmitted to the new model. So the question arises whether manual labeling of the custom dataset would bring better results.

- Transfer learning has many advantages for training neural networks. Most of the core models, like `ResNet34`, are trained on `ImageNet` dataset. Images in `ImageNet` archive have different semantic content that Earth Observation images; Multi-spectral data have a higher number of dimensions (bands); There are differences in spatial resolution between computer vision images and remote sensing images. Using core models trained on remote sensing datasets, such as `BigEarthNet`[1] can significantly improve results.

- Only one architecture (`Unet` with `ResNet34` backbone) and one metric was used for image segmentation. The possibilities of image segmentation were only illustrated and more architectures with different metrics should be compared.

[1] http://bigearth.net/

Chapter 6

Conclusion

The main goal of the thesis was to identify and apply different techniques for deforestation detection from satellite imagery.

This thesis has shown how to access, download, and analyze satellite data for forest change detection. It explains the specifics of Earth Observation imagery, what to watch out for during data pre-processing, and covered different techniques that are trying to achieve the same goal - to detect deforestation.

We were able to successfully conduct all experiments, but with different results. All methods can be further evaluated, as outlined in the discussion.

NDVI change detection method is susceptible to have properly cleared of clouds. If the clouds were not filtered, the results would be unusable. Because the method compares two different periods, it is not possible to say exactly when the land cover change occurred.

Neural Network with Unet architecture performed basic image segmentation. Like most of the neural networks, our model is heavily dependent on the quality and size of the training dataset. Even with the relatively small dataset, it was still able to learn features and shapes of deforested patches, although the final accuracy in the metric was low. Evaluating detection results with the human eye uncovers that the network was able to detect deforested patches, that were not in the training dataset. The neural network model has the biggest potential for future improvement.

The biggest advantage of analytical methods that are working with radar data is that are weather independent and can detect changes as often as new satellite acquisition is available. The drawback is that we need to be careful to choose correct parameters when selecting the data to download and during pre-processing. Choosing different thresholds in analytical methods can have a big impact on results and what are these results representing.

Bibliography

[1] Agency, E. E. *Natura2000 site SKCHVU050*. 2020 [cit. 2020-07-30]. Available at: https://natura2000.eea.europa.eu/Natura2000/SDF.aspx?site=SKCHVU050.

[2] community, S. *NumPy Documentation*. 2020 [cit. 2020-07-30]. Available at: https://numpy.org/doc/stable/.

[3] Copernicus. *Copernicus Access to Data*. 2020 [cit. 2020-07-30]. Available at: https://www.copernicus.eu/en/access-data.

[4] EOS. *Natural color*. 2020 [cit. 2020-07-30]. Available at: https://eos.com/natural-color/.

[5] ESA. *Sentinel-1 SAR Definitions*. 2020 [cit. 2020-07-30]. Available at: https://sentinel.esa.int/web/sentinel/user-guides/sentinel-1-sar/definitions.

[6] ESA. *Sentinel-2 MSI Introduction*. 2020 [cit. 2020-07-30]. Available at: https://sentinel.esa.int/web/sentinel/user-guides/sentinel-2-msi.

[7] ESA/ATGmedialab. *Sentinel-1 radar vision*. 2014 [cit. 2020-05-24]. Available at: http://www.esa.int/ESA_Multimedia/Images/2014/01/Sentinel-1_radar_vision.

[8] EUROPE, F. *State of Europe's Forests 2015* [online]. 2015 [cit. 2020-05-24]. Available at: https://foresteurope.org/state-europes-forests-2015-report/.

[9] fast.ai. *Fastai Documentation*. 2020 [cit. 2020-07-30]. Available at: https://docs.fast.ai/.

[10] Flores, A., Herndon, K., Thapa, R. and Cherrington, E. *The SAR Handbook: Comprehensive Methodologies for Forest Monitoring and Biomass Estimation* [electronically]. 1st ed. April 2019 [cit. 2020-05-24]. Available at: https://gis1.servirglobal.net/TrainingMaterials/SAR/SARHB_FullRes.pdf.

[11] Frank Warmerdam, E. R. *GDAL Documentation*. 2020 [cit. 2020-07-30]. Available at: https://gdal.org/.

[12] Geopandas. *Geopandas documentation*. 2020 [cit. 2020-07-30]. Available at: https://geopandas.org.

[13] Hansen, M. C., Potapov, P. V., Moore, R., Hancher, M., Turubanova, S. A. et al. *High-Resolution Global Maps of 21st-Century Forest Cover Change.* [online]. 2013 [cit. 2020-05-24]. Available at: http://earthenginepartners.appspot.com/science-2013-global-forest.

[14] IETF. *RFC7946 GeoJSON*. 2016 [cit. 2020-07-30]. Available at: https://tools.ietf.org/html/rfc7946.

[15] Janssen, V. Understanding coordinate reference systems, datums and transformations. *International Journal of Geoinformatics*. january 2009, vol. 5.

[16] Mapbox. *Rasterio Documentation*. 2018 [cit. 2020-07-30]. Available at: https://rasterio.readthedocs.io/en/latest/.

[17] NASA. *Normalized Difference Vegetation Index (NDVI)*. 2000 [cit. 2020-07-30]. Available at: https://earthobservatory.nasa.gov/features/MeasuringVegetation/measuring_vegetation_2.php.

[18] NASA. *Why Space Radiation Matters*. 2019 [cit. 2020-07-30]. Available at: https://www.nasa.gov/analogs/nsrl/why-space-radiation-matters.

[19] OGC. *OGC GeoTIFF Standard*. 2020 [cit. 2020-07-30]. Available at: https://www.ogc.org/standards/geotiff.

[20] Ronneberger, O., Fischer, P. and Brox, T. U-Net: Convolutional Networks for Biomedical Image Segmentation. *CoRR*. 2015, abs/1505.04597. Available at: http://arxiv.org/abs/1505.04597.

[21] Sean Gillies, K. L. *Shapely Documentation*. 2013 [cit. 2020-07-30]. Available at: https://shapely.readthedocs.io/en/latest/index.html.

[22] Sinergise. *Eo-learn documentation*. 2020 [cit. 2020-07-30]. Available at: https://eo-learn.readthedocs.io/en/latest/.

[23] SINERGISE. *Sentinel Hub documentation* [online]. 2020. 2020-05-24 [cit. 2020-05-24]. Available at: https://docs.sentinel-hub.com/api/latest/#/.

[24] Sinergise. *Sentinelhub documentation*. 2020 [cit. 2020-07-30]. Available at: https://sentinelhub-py.readthedocs.io/en/latest.

Appendix A

Contents of the included storage media

- **doc** - LaTeX source code of technical report and generated PDF.
- **models** - Saved models of trained neural networks
- **data** - Dataset
- **src** - Source code files used for this thesis